

A Jensen-Shannon Divergence Based Loss Function for Bayesian Neural Networks

Ponkrshnan Thiagarajan ^{a,1}, Susanta Ghosh ^{b,2}

^aDepartment of Mechanical Engineering-Engineering Mechanics, Michigan Technological University, MI, USA

^bMechanical Engineering-Engineering Mechanics and the Institute of Computing and Cybersystems, Michigan Technological University, MI, USA.

Abstract

Kullback-Leibler (KL) divergence is widely used for variational inference of Bayesian Neural Networks (BNNs). However, the KL divergence has limitations such as unboundedness and asymmetry. We examine the Jensen-Shannon (JS) divergence that is more general, bounded, and symmetric. We formulate a novel loss function for BNNs based on the geometric JS divergence and show that the conventional KL divergence-based loss function is its special case. We evaluate the divergence part of the proposed loss function in a closed form for a Gaussian prior. For any other general prior, Monte Carlo approximations can be used. We provide algorithms for implementing both of these cases. We demonstrate that the proposed loss function offers an additional parameter that can be tuned to control the degree of regularisation. We derive the conditions under which the proposed loss function regularises better than the KL divergence-based loss function for Gaussian priors and posteriors. We demonstrate performance improvements over the state-of-the-art KL divergence-based BNN on the classification of a noisy CIFAR data set and a biased histopathology data set.

Keywords: Bayesian convolutional neural networks, Variational inference, KL divergence, JS divergence, Uncertainty quantification.

1. Introduction

Despite the wide use and success of deep and convolutional neural networks in numerous science and engineering applications [1–10], they suffer from overfitting when the data set is small, noisy or biased [11]. Further, due to a very large number of (deterministic) parameters, CNNs cannot provide a robust measure of uncertainty. Without a measure of uncertainty, erroneous predictions by these models can lead to catastrophic results in applications such as autonomous driving or medical diagnosis. In the past, several methods were developed to provide prediction intervals as a measure of uncertainty in neural networks. Some of these include the delta method, bootstrap method, mean-variance estimation method, Bayesian method, etc. [12]. Amongst these different methods for uncertainty quantification, Bayesian methods have gained popularity due to their rigorous mathematical foundation for quantifying uncertainties through their stochastic parameters [12, 13]. In the following, key aspects of Bayesian Neural Networks (BNNs) are briefly summarised.

Bayesian Neural Networks: In a Bayesian neural network, the parameters are treated as random variables, and the distributions of these parameters are learned from the training data. The first known BNN developed by Tishby et al [14] showed that the posterior distributions of weights and biases can be obtained via the Bayes rule from chosen priors. Though their work provided theoretical insights, a method to perform inference was still not available.

¹email: thiagara@mtu.edu

²email: susantag@mtu.edu

This paper is to be submitted in IEEE for peer review.

We acknowledge Superior, a high-performance computing facility at MTU. This work used the XSEDE Bridges at the Pittsburgh Supercomputing Center through allocation No. MSS200004.

Following this work, Laplace approximations were proposed to perform inference on the posterior distribution of weights by Denker and LeCun [15]. For a detailed account on BNN see the reviews [16, 17]. The two most commonly used techniques to approximate the posterior distribution of weights of a BNN are the Variational Inference (VI) and the Markov Chain Monte Carlo Methods (MCMC). A brief review of some of the early works on these two techniques is presented in the following.

Variational Inference in Bayesian Neural Networks: Minimum description length (MDL) was used to penalize the information contained in network weights to address the problem of overfitting by Hinton and Van Camp [18]. Though their method was based on the foundations of information theory, the resulting framework closely resembled VI (described in Sec.2.2). In their work, the posterior distribution of weights was assumed to be a factorization of independent Gaussians. The well-known strong correlation between the network parameters was neglected. As an extension to their work, a full correlation between the network parameters was introduced by Barber and Bishop [19] leading to full covariance matrices instead of the diagonal covariance matrices in [18]. Despite the advantages, the methods [18, 19] focused on developing closed-form representations of networks and were limited to single hidden layer networks. With the development of larger networks, these closed-form representations failed as the number of parameters increased drastically with the addition of more and more deep layers. Another alternative to approximating the posterior distribution is the MCMC technique.

Markov Chain Monte Carlo Methods for Bayesian Neural Networks: MCMC methods comprise a set of algorithms to sample from arbitrary and intractable distributions. MCMC approaches can converge very closely to the true posterior but these approaches are computationally demanding. The potential of the Hamiltonian Monte Carlo technique in the context of Bayesian inference was explored by Neal [20]. Their method performed very well for the inference of small Bayesian models but failed to scale for larger models. To overcome this difficulty, a Langevin method named Stochastic Gradient Langevin Dynamics was introduced by Welling and Teh [21] that scaled well for large models. Despite these advancements, MCMC techniques require huge computational efforts.

Recent Advances on Bayesian Neural Networks: Computational cost was a bottleneck to BNN research in the late 90s. With the advancement in GPU computation, research in the field of BNN resurged. A data sub-sampling technique to scale for large amounts of data in a VI objective was proposed by Graves [22]. Their method maximized the expected lower bound (ELBO) on the marginal likelihood to learn the network parameters. The Expected log-likelihood was approximated using Monte Carlo estimates allowing the method to scale for large networks. While their method [22] enabled the application of VI for large networks, its implementation showed poor performance due to high variance in the gradient computations during Monte Carlo approximation and due to a lack of correlations between weights. An algorithm to implement back-propagation for stochastic parameters was proposed by Hernandez et al [23] to improve upon the VI approaches proposed by Graves [22]. An efficient method for VI known as *Bayes by Backprop* was introduced by Blundell et al. [24] that extends Graves' [22] approach. Their work uses a re-parameterization trick [25, 26] that separates the stochastic variables to facilitate back-propagation.

To summarise the above literature, inference of posterior using MCMC algorithms can be very accurate but they are computationally demanding. In addition, MCMC algorithms do not scale well with the model size. Whereas VI methods are efficient and scalable techniques that provide an approximate inference of the posterior. Given the huge size of modern Bayesian networks, VI appears to be the most suitable and thus widely used. Most of the VI technique in the literature uses the KL divergence as a measure of dissimilarity between the true and approximate posteriors. However, the KL divergence has limitations such as asymmetric property and unboundedness. These limitations may lead to poor generalization or failure during training as reported in [27]. Therefore it is imperative to explore alternative divergences for VI that can alleviate these limitations. Although other approximate inference techniques based on α -divergence minimization [28–30] have been investigated, no significant progress has been made in this direction.

Proposed Jensen-Shannon Divergence based Loss Function for Bayesian Neural Networks: In this work, we present a Jensen-Shannon divergence-based constrained optimization problem that results in a novel loss function for BNNs. This loss function can be considered as a generalization to the ELBO loss obtained by variance inference of the posterior using KL divergence. We show that the ELBO loss [22–24] is a special case of the loss function proposed in this work. In addition, we show that the loss function presented in this work performs better on classification problems where the dataset is noisy or is biased towards a particular class. Further, we derive the conditions under which the proposed JS divergence-based loss function regularises better than the KL divergence-based loss function for Gaussian priors and posteriors.

The rest of the manuscript is organized as follows: Sec. 2 describes the proposed loss function. The details of the numerical experiments are provided in Sec. 3. The results obtained by the present method are presented and discussed in Sec. 4. Finally, the conclusion is provided in Sec. 5.

2. Methods

2.1. Background: KL and JS divergences

Consider two random variables \mathcal{P} and \mathcal{Q} defined on a probability space \mathcal{X} . The KL divergence between \mathcal{P} and \mathcal{Q} is defined as

$$\text{KL}[\mathcal{P} \parallel \mathcal{Q}] = \int_{\mathcal{X}} p(x) \log \left[\frac{p(x)}{q(x)} \right] dx \quad (1)$$

where $p(x)$ and $q(x)$ are the probability densities of \mathcal{P} and \mathcal{Q} respectively. For two n-dimensional multivariate Gaussian distributions³ $\mathcal{N}_1(\mu_1, \Sigma_1)$ and $\mathcal{N}_2(\mu_2, \Sigma_2)$, the KL divergence is given by

$$\text{KL}(\mathcal{N}_1 \parallel \mathcal{N}_2) = \frac{1}{2} \left[\text{tr}(\Sigma_2^{-1} \Sigma_1) + \ln \frac{|\Sigma_2|}{|\Sigma_1|} + (\mu_2 - \mu_1)^T \Sigma_2^{-1} (\mu_2 - \mu_1) - n \right] \quad (2)$$

The KL divergence is widely used in literature to represent the dissimilarity between two probability distributions for various applications such as VI. However, it has limitations such as the asymmetric property i.e $\text{KL}[\mathcal{P} \parallel \mathcal{Q}] \neq \text{KL}[\mathcal{Q} \parallel \mathcal{P}]$, and unboundedness. These limitations may lead to difficulty in approximating light-tailed posteriors as reported in [27].

To overcome these limitations a symmetric JS divergence can be employed. JS divergence is defined as

$$\text{JS}[\mathcal{P} \parallel \mathcal{Q}] = \frac{1}{2} \text{KL} \left[p \parallel \frac{p+q}{2} \right] + \frac{1}{2} \text{KL} \left[q \parallel \frac{p+q}{2} \right] \quad (3)$$

Although this JS divergence is symmetric and bounded, unlike the KL divergence its closed-form expression cannot be obtained even when p and q are Gaussians. This difficulty is due to the fact that there is a term in Eq. (3) that involves a sum of p and q which cannot be expressed in a closed form. To overcome this lack of closed-form expression for JS divergence a generalization of the JS divergence using abstract means, specifically the geometric mean was proposed by Nielsen [31]. By considering the weighted geometric mean of two variables x and y ,

$$G_\alpha(x, y) = x^{1-\alpha} y^\alpha; \quad \alpha \in [0, 1] \quad (4)$$

the following new family of skew-symmetric geometric divergence has been introduced in [31],

$$\text{JS}^{G_\alpha}[\mathcal{P} \parallel \mathcal{Q}] = (1 - \alpha) \text{KL}(p \parallel G_\alpha(p, q)) + \alpha \text{KL}(q \parallel G_\alpha(p, q)) \quad (5)$$

The α parameter in Eq. (5) is a skew parameter that controls the divergence skew between p and q . The fact that the weighted product of exponential family distributions stays in the exponential family was utilized to derive a closed form solution for (JS^{G_α}) of multivariate Gaussian distributions. For, $N_1 \sim \mathcal{N}(\mu_1, \Sigma_1)$ and $N_2 \sim \mathcal{N}(\mu_2, \Sigma_2)$, the JS^{G_α} is given by

$$\begin{aligned} \text{JS}^{G_\alpha}(N_1 \parallel N_2) &= (1 - \alpha) \text{KL}(N_1 \parallel N_\alpha) + \alpha \text{KL}(N_2 \parallel N_\alpha) \\ &= \frac{1}{2} \left[\text{tr} \left(\frac{(1 - \alpha) \Sigma_1 + \alpha \Sigma_2}{\Sigma_\alpha} \right) + \log \left(\frac{|\Sigma_\alpha|}{|\Sigma_1|^{1-\alpha} |\Sigma_2|^\alpha} \right) + (1 - \alpha) (\mu_\alpha - \mu_1)^T \Sigma_\alpha^{-1} (\mu_\alpha - \mu_1) + \right. \\ &\quad \left. \alpha (\mu_\alpha - \mu_2)^T \Sigma_\alpha^{-1} (\mu_\alpha - \mu_2) - n \right] \end{aligned} \quad (6)$$

where the intermediate mean distribution $N_\alpha \sim \mathcal{N}(\mu_\alpha, \Sigma_\alpha)$ has the following parameters,

$$\Sigma_\alpha = \left[(1 - \alpha) \Sigma_1^{-1} + \alpha \Sigma_2^{-1} \right]^{-1} \quad \mu_\alpha = \Sigma_\alpha \left[(1 - \alpha) \Sigma_1^{-1} \mu_1 + \alpha \Sigma_2^{-1} \mu_2 \right] \quad (7)$$

³ \mathcal{N} denotes a Gaussian distribution throughout this work.

However, the skew-symmetric divergence in Eq.(5) fails to capture the divergence between p and q in the limits of α since,

$$\left[\text{JS}^{G_\alpha}(\mathcal{P} \parallel \mathcal{Q}) \right]_{\alpha=0} = 0 \qquad \left[\text{JS}^{G_\alpha}(\mathcal{P} \parallel \mathcal{Q}) \right]_{\alpha=1} = 0 \quad (8)$$

which is an unacceptable property of a divergence. To resolve this issue, Deasy et al. [32] used the geometric mean

$$G'_\alpha(x, y) = x^\alpha y^{1-\alpha}; \quad \alpha \in [0, 1] \quad (9)$$

to implement JS divergence in variational autoencoders. This reverse form of geometric mean (Eq. (9)) yields KL divergences in the limiting values of the skew parameter, as given below:

$$\left[\text{JS}^{G'_\alpha}(\mathcal{P} \parallel \mathcal{Q}) \right]_{\alpha=0} = \text{KL}(\mathcal{P} \parallel \mathcal{Q}) \qquad \left[\text{JS}^{G'_\alpha}(\mathcal{P} \parallel \mathcal{Q}) \right]_{\alpha=1} = \text{KL}(\mathcal{P} \parallel \mathcal{Q}) \quad (10)$$

For two multivariate Gaussian distributions, the JS divergence with the reverse form of the geometric mean can be written as

$$\text{JS}^{G'_\alpha}(N_1 \parallel N_2) = (1 - \alpha)\text{KL}(N_1 \parallel N'_\alpha) + \alpha\text{KL}(N_2 \parallel N'_\alpha) \quad (11)$$

where, $N'_\alpha \sim \mathcal{N}(\mu'_\alpha, \Sigma'_\alpha)$ is an intermediate mean distribution with the parameters

$$\Sigma'_\alpha = \left[\alpha \Sigma_1^{-1} + (1 - \alpha) \Sigma_2^{-1} \right]^{-1} \qquad \mu'_\alpha = \Sigma_\alpha \left[\alpha \Sigma_1^{-1} \mu_1 + (1 - \alpha) \Sigma_2^{-1} \mu_2 \right] \quad (12)$$

2.2. Background: Variational inference

Given a set of training data $\mathbb{D} = \{\mathbf{x}_n, \mathbf{y}_n\}_{n=1}^N$ and a test input, we are interested in learning a data-driven model (for instance a BNN) to predict the probability of output $P(\mathbf{y}|\mathbf{x}, \mathbb{D})$. Where $\mathbf{y} \in \Upsilon$ is the output for a given test input $\mathbf{x} \in \mathbb{R}^p$ and Υ is the output space. To this end we train a neural network with random parameters \mathbf{w} and learn the probability distribution of these parameters $P(\mathbf{w}|\mathbb{D})$ from the training data \mathbb{D} using the Bayes' rule as follows:

$$P(\mathbf{w}|\mathbb{D}) = \frac{P(\mathbb{D}|\mathbf{w})P(\mathbf{w})}{P(\mathbb{D})} \quad (13)$$

The term $P(\mathbb{D}|\mathbf{w})$ is the likelihood of the training data \mathbb{D} given a parameter setting \mathbf{w} . Assuming each training data to be independent and identically distributed, the above term becomes the product of likelihood,

$$P(\mathbb{D}|\mathbf{w}) = \prod_{n=1}^N P(\mathbf{y}_n|\mathbf{w}, \mathbf{x}_n) \quad (14)$$

The prior $P(\mathbf{w})$ is our belief about the distribution of weights before seeing the data. The term $P(\mathbb{D})$ involves marginalization over the weight distribution:

$$P(\mathbb{D}) = \int_{\Omega_{\mathbf{w}}} P(\mathbb{D}|\mathbf{w})P(\mathbf{w})d\mathbf{w} \quad (15)$$

Once we obtain the posterior distribution of weights as shown in Eq. (13), the predictive distribution can be obtained by marginalizing over the weights as

$$P(\mathbf{y}|\mathbf{x}, \mathbb{D}) = \int_{\Omega_{\mathbf{w}}} P(\mathbf{y}|\mathbf{x}, \mathbf{w})P(\mathbf{w}|\mathbb{D})d\mathbf{w} \quad (16)$$

The term $P(\mathbb{D})$ in Eq. (13) is intractable due to marginalization over \mathbf{w} , which in turn makes the posterior distribution of weights $P(\mathbf{w}|\mathbb{D})$ intractable. Thus, the posterior is approximated using variational inference.

In variational inference, the unknown intractable posterior $P(\mathbf{w}|\mathbb{D})$ is approximated by a known simpler distribution $q(\mathbf{w}|\boldsymbol{\theta})$ over the model weights. This simpler distribution is referred to as the variational posterior, which can be defined by a set of parameters $\boldsymbol{\theta}$. For example, if q is assumed to be a Gaussian distribution then the parameters $\boldsymbol{\theta}$ are the mean

μ and the standard deviation σ . In variational inference, the set of parameters θ for the model weights is learned by minimizing the KL divergence between the true posterior P and approximate posterior q as shown in [24].

$$\theta^* = \arg \min_{\theta} \text{KL} [q(\mathbf{w}|\theta) \parallel P(\mathbf{w}|\mathbb{D})] \quad (17)$$

The cost function $\mathcal{F}(\mathbb{D}, \theta)$ is minimised to learn the optimal parameters θ^* . $\mathcal{F}(\mathbb{D}, \theta)$ is expressed as:

$$\begin{aligned} \mathcal{F}(\mathbb{D}, \theta) &= \text{KL} [q(\mathbf{w}|\theta) \parallel P(\mathbf{w}|\mathbb{D})] \\ &= \int q(\mathbf{w}|\theta) \log \frac{q(\mathbf{w}|\theta)}{P(\mathbf{w})P(\mathbb{D}|\mathbf{w})} d\mathbf{w} \\ &= \text{KL} [q(\mathbf{w}|\theta) \parallel P(\mathbf{w})] - \mathbb{E}_{q(\mathbf{w}|\theta)}[\log P(\mathbb{D}|\mathbf{w})] \end{aligned} \quad (18)$$

The term $P(\mathbb{D})$ is ignored in Eq. (18) since it is a constant and does not affect the optimization. This cost function Eq. (18) is known as the variational free energy or evidence lower bound. This cost function is minimized to learn the set of parameters θ .

2.3. Proposed formulation: JS divergence based Loss function

2.3.1. Intractability of the JS based variational inference

We propose to use the more general JS divergence as a measure of dissimilarity between the true posterior $P(\mathbf{w}|\mathbb{D})$ and the variational posterior $q(\mathbf{w}|\theta)$ in Eq. (17). Therefore, the optimization problem becomes,

$$\theta^* = \arg \min_{\theta} \text{JS}^{G_{\alpha}} [q(\mathbf{w}|\theta) \parallel P(\mathbf{w}|\mathbb{D})] \quad (19)$$

The cost function can then be written as,

$$\begin{aligned} \hat{\mathcal{F}}(\mathbb{D}, \theta) &= \text{JS}^{G_{\alpha}} [q(\mathbf{w}|\theta) \parallel P(\mathbf{w}|\mathbb{D})] \\ &= (1 - \alpha)\text{KL} (q \parallel G'_{\alpha}(q, P)) + \alpha\text{KL} (P \parallel G'_{\alpha}(q, P)) \end{aligned} \quad (20)$$

Where, $G'_{\alpha}(q, P) = q(\mathbf{w}|\theta)^{\alpha} P(\mathbf{w}|\mathbb{D})^{(1-\alpha)}$.

Let us rewrite the first term in Eq. (20) as,

$$\begin{aligned} T_1 &= (1 - \alpha)\text{KL} (q \parallel G'_{\alpha}(q, P)) \\ &= (1 - \alpha)\text{KL}[q(\mathbf{w}|\theta) \parallel q(\mathbf{w}|\theta)^{\alpha} P(\mathbf{w}|\mathbb{D})^{(1-\alpha)}] \\ &= (1 - \alpha) \int q(\mathbf{w}|\theta) \log \left[\frac{q(\mathbf{w}|\theta)}{q(\mathbf{w}|\theta)^{\alpha} P(\mathbf{w}|\mathbb{D})^{1-\alpha}} \right] d\mathbf{w} \\ &= (1 - \alpha)^2 \int q(\mathbf{w}|\theta) \log \left[\frac{q(\mathbf{w}|\theta)}{P(\mathbf{w}|\mathbb{D})} \right] d\mathbf{w} \end{aligned} \quad (21)$$

Note that, this term is equivalent to loss function in Eq. (18) multiplied by a constant $(1 - \alpha)^2$. Similarly let us rewrite the second term in Eq. (20) as,

$$\begin{aligned} T_2 &= \alpha\text{KL} (P \parallel G'_{\alpha}(q, P)) \\ &= \alpha\text{KL}[P(\mathbf{w}|\mathbb{D}) \parallel q(\mathbf{w}|\theta)^{\alpha} P(\mathbf{w}|\mathbb{D})^{(1-\alpha)}] \\ &= \alpha \int P(\mathbf{w}|\mathbb{D}) \log \left[\frac{P(\mathbf{w}|\mathbb{D})}{q(\mathbf{w}|\theta)^{\alpha} P(\mathbf{w}|\mathbb{D})^{(1-\alpha)}} \right] d\mathbf{w} \\ &= \alpha^2 \int P(\mathbf{w}|\mathbb{D}) \log \left[\frac{P(\mathbf{w}|\mathbb{D})}{q(\mathbf{w}|\theta)} \right] d\mathbf{w} \end{aligned} \quad (22)$$

The term $P(\mathbf{w}|\mathbb{D})$ in Eq. (22) is intractable as explained in section 2.2 which makes T_2 intractable. Therefore the cost function Eq. (20) cannot be used to find the optimum parameter θ^* which contrasts the KL divergence based loss function in Eq. (18).⁴ To overcome this challenge, we propose to derive a loss function for BNNs in a constrained optimization framework. We start from the likelihood of observing the data and show its equivalency to the loss function obtained through variational inference.

⁴We obtain a similar result when the geometric mean G_{α} is used. Only the constants outside the integral change in that case.

2.3.2. Loss function derived using a constrained optimisation framework

Following the constrained optimization framework present in the literature for variational autoencoders [32, 33], we derive the loss function for BNNs. Given a set of training data \mathbb{D} , we are interested in learning the probability distribution of weights of the neural network such that, the likelihood of observing the data given the weights is maximized. Thus, the optimization problem can be written as

$$\max_{\theta} \mathbb{E}_{q(\mathbf{w}|\theta)} [\log P(\mathbb{D}|\mathbf{w})] \quad (23)$$

Where θ is a set of parameters of the inferred probability distribution q . This probability distribution q is constrained with a prior on the parameters, $P(\mathbf{w})$, to regularise the parameters. This leads to a constrained optimization problem as given below:

$$\max_{\theta} \mathbb{E}_{q(\mathbf{w}|\theta)} [\log P(\mathbb{D}|\mathbf{w})] \quad \text{subject to } D(q(\mathbf{w}|\theta) \| P(\mathbf{w})) < \epsilon \quad (24)$$

where ϵ determines the strength of the applied constraint and D is a divergence measure. The constrained optimization problem Eq. (24) can be re-written as a Lagrangian following the KKT approach as,

$$\mathcal{L} = \mathbb{E}_{q(\mathbf{w}|\theta)} [\log P(\mathbb{D}|\mathbf{w})] - \lambda(D(q(\mathbf{w}|\theta) \| P(\mathbf{w})) - \epsilon) \quad (25)$$

Maximizing \mathcal{L} leads to the learning of weights. Here ϵ is a constant which can be removed from the optimization. Also changing the sign of the above equations leads to the cost function that needs to be minimized.

$$\tilde{\mathcal{F}} = \lambda D(q(\mathbf{w}|\theta) \| P(\mathbf{w})) - \mathbb{E}_{q(\mathbf{w}|\theta)} [\log P(\mathbb{D}|\mathbf{w})] \quad (26)$$

Considering the KL divergence as the divergence measure and $\lambda = 1$ reproduces the cost function given by Blundell et al [24].

2.3.3. J-S divergence

We propose to use the J-S divergence as the divergence measure, D , in Eq.(26) which leads to the following loss function:

$$\begin{aligned} \tilde{\mathcal{F}}'_{js} &= \lambda \text{JS}^{G'_\alpha}(q(\mathbf{w}|\theta) \| P(\mathbf{w})) - \mathbb{E}_{q(\mathbf{w}|\theta)} [\log P(\mathbb{D}|\mathbf{w})] \\ &= \lambda(1 - \alpha) \text{KL}(q \| G'_\alpha(q, P_w)) + \lambda\alpha \text{KL}(P_w \| G'_\alpha(q, P_w)) - \mathbb{E}_{q(\mathbf{w}|\theta)} [\log P(\mathbb{D}|\mathbf{w})] \end{aligned} \quad (27)$$

Further,

$$\begin{aligned} \text{KL}(q \| G'_\alpha(q, P_w)) &= \int q(\mathbf{w}|\theta) \log \frac{q(\mathbf{w}|\theta)}{q(\mathbf{w}|\theta)^\alpha P(\mathbf{w})^{1-\alpha}} d\mathbf{w} \\ &= (1 - \alpha) \int q(\mathbf{w}|\theta) \log \frac{q(\mathbf{w}|\theta)}{P(\mathbf{w})} d\mathbf{w} \end{aligned} \quad (28)$$

and

$$\begin{aligned} \text{KL}(P_w \| G'_\alpha(q, P_w)) &= \int P(\mathbf{w}) \log \frac{P(\mathbf{w})}{q(\mathbf{w}|\theta)^\alpha P(\mathbf{w})^{1-\alpha}} d\mathbf{w} \\ &= \alpha \int P(\mathbf{w}) \log \frac{P(\mathbf{w})}{q(\mathbf{w}|\theta)} d\mathbf{w} \end{aligned} \quad (29)$$

From Eq. (27) – Eq. (29) we have,

$$\tilde{\mathcal{F}}'_{js} = \lambda(1 - \alpha)^2 \int q(\mathbf{w}|\theta) \log \frac{q(\mathbf{w}|\theta)}{P(\mathbf{w})} d\mathbf{w} + \lambda\alpha^2 \int P(\mathbf{w}) \log \frac{P(\mathbf{w})}{q(\mathbf{w}|\theta)} d\mathbf{w} - \mathbb{E}_{q(\mathbf{w}|\theta)} [\log P(\mathbb{D}|\mathbf{w})] \quad (30)$$

Eq. (30) can be written in terms of expectations as,

$$\tilde{\mathcal{F}}'_{js} = \lambda(1 - \alpha)^2 \mathbb{E}_{q(\mathbf{w}|\boldsymbol{\theta})} \left[\log \frac{q(\mathbf{w}|\boldsymbol{\theta})}{P(\mathbf{w})} \right] + \lambda\alpha^2 \mathbb{E}_{P(\mathbf{w})} \left[\log \frac{P(\mathbf{w})}{q(\mathbf{w}|\boldsymbol{\theta})} \right] - \mathbb{E}_{q(\mathbf{w}|\boldsymbol{\theta})} [\log P(\mathbb{D}|\mathbf{w})] \quad (31)$$

In Eq.(30), the first term is the the mean seeking forward KL divergence $\text{KL}(P(\mathbf{w})||q(\mathbf{w}|\boldsymbol{\theta}))$ and the second term is the mode seeking reverse KL divergence $\text{KL}^*(P(\mathbf{w})||q(\mathbf{w}|\boldsymbol{\theta}))$. Thus, the JS divergence-based loss function is a weighted sum of the forward and reverse KL divergence of the prior and the variational posterior. Further, the first and last terms of the above loss function, Eq. (30), are the same as the loss function obtained by variational inference. Therefore, as we derive this loss function by constraining the maximum likelihood function, we have an additional term in addition to the loss function provided by the variational inference. This additional term should ensure better regularisation by imposing stricter penalization if the posterior is away from the prior distribution. This fact will be demonstrated via numerical results in Sec. 2.6.1. And the additional parameters λ and α should provide better control on the amount of regularisation.

Remark: The above loss function, Eq. (30), is derived considering the reverse geometric mean $G'_\alpha(x, y) = x^\alpha y^{1-\alpha}$ proposed in [32]. If we consider the geometric mean $G_\alpha(x, y) = x^{1-\alpha} y^\alpha$, the cost function is,

$$\tilde{\mathcal{F}}_s = \lambda\alpha(1 - \alpha) \left[\int q(\mathbf{w}|\boldsymbol{\theta}) \log \frac{q(\mathbf{w}|\boldsymbol{\theta})}{P(\mathbf{w})} d\mathbf{w} + \int P(\mathbf{w}) \log \frac{P(\mathbf{w})}{q(\mathbf{w}|\boldsymbol{\theta})} d\mathbf{w} \right] - \mathbb{E}_{q(\mathbf{w}|\boldsymbol{\theta})} [\log P(\mathbb{D}|\mathbf{w})] \quad (32)$$

2.4. Minimisation of the loss function in a closed-form for Gaussian priors

In this subsection, we describe the minimization of the loss functions in closed-form for Gaussian priors. The closed form expression is presented in Sec.2.3.2. Let us consider the prior and the likelihood follows the Gaussian distribution and hence the posterior also follows the Gaussian distribution. The Gaussian prior is denoted by $P_N(\mathbf{w}) \sim \mathcal{N}(\boldsymbol{\mu}_1, \boldsymbol{\sigma}_1^2)$ and the Gaussian posterior is denoted as $q_N(\mathbf{w}|\boldsymbol{\theta}) \sim \mathcal{N}(\boldsymbol{\mu}_2, \boldsymbol{\sigma}_2^2)$, where the subscript $(\cdot)_N$ indicates Gaussian distribution. $\boldsymbol{\mu}_1$ and $\boldsymbol{\mu}_2$ are n-dimensional vectors and $\boldsymbol{\sigma}_1^2, \boldsymbol{\sigma}_2^2$ are diagonal matrices such that $\boldsymbol{\mu}_1 = [\mu_{11}, \mu_{12}, \dots, \mu_{1n}]^T$ and $\boldsymbol{\sigma}_1^2 = \text{diag}(\sigma_{11}^2, \sigma_{12}^2, \dots, \sigma_{1n}^2)$ (similarly for $\boldsymbol{\mu}_2$ and $\boldsymbol{\sigma}_2^2$). The JS divergence ($\text{JS}^{G'_\alpha}$) can be written as,

$$\text{JS}^{G'_\alpha}(q_N||P_N) = \frac{1}{2} \sum_{i=1}^n \left[\frac{(1 - \alpha)\sigma_{1i}^2 + \alpha\sigma_{2i}^2}{\sigma_{ai}^2} + \log \frac{(\sigma'_{ai})^2}{\sigma_{1i}^{2(1-\alpha)} \sigma_{2i}^{2\alpha}} + (1 - \alpha) \frac{(\mu'_{ai} - \mu_{1i})^2}{(\sigma'_{ai})^2} + \frac{\alpha(\mu'_{ai} - \mu_{2i})^2}{(\sigma'_{ai})^2} - 1 \right] \quad (33)$$

where,

$$(\sigma'_{ai})^2 = \frac{\sigma_{1i}^2 \sigma_{2i}^2}{(1 - \alpha)\sigma_{1i}^2 + \alpha\sigma_{2i}^2} \quad \mu'_{ai} = (\sigma'_{ai})^2 \left[\frac{\alpha\mu_{1i}}{\sigma_{1i}^2} + \frac{(1 - \alpha)\mu_{2i}}{\sigma_{2i}^2} \right] \quad (34)$$

Therefore, the divergence term of the proposed loss function (Eq. (27)) can be replaced by this closed form expression given in Eq. (33). The second term, which is the expectation of the log-likelihood ($\mathbb{E}_{q(\mathbf{w}|\boldsymbol{\theta})} [\log P(\mathbb{D}|\mathbf{w})]$) can be approximated by a Monte-Carlo sampling as shown in the algorithm 1. Where, $\boldsymbol{\theta} = (\boldsymbol{\mu}, \boldsymbol{\rho})$ are the parameters of the posterior distribution of weights that we wish to learn. Here, the reparametrisation trick is used to separate the deterministic and the stochastic variables.

Remark:

For Gaussian priors, a closed form expression can be obtained similarly for JS divergence using the geometric mean G_α which gives,

$$\text{JS}^{G_\alpha}(N_1||N_2) = \frac{1}{2} \sum_{i=1}^n \left[\frac{(1 - \alpha)\sigma_{1i}^2 + \alpha\sigma_{2i}^2}{\sigma_{ai}^2} + \log \frac{\sigma_{ai}^2}{\sigma_{1i}^{2(1-\alpha)} \sigma_{2i}^{2\alpha}} + (1 - \alpha) \frac{(\mu_{ai} - \mu_{1i})^2}{\sigma_{ai}^2} + \frac{\alpha(\mu_{ai} - \mu_{2i})^2}{\sigma_{ai}^2} - 1 \right] \quad (35)$$

with the parameters,

$$\sigma_{ai}^2 = \frac{\sigma_{1i}^2 \sigma_{2i}^2}{\alpha\sigma_{1i}^2 + (1 - \alpha)\sigma_{2i}^2} \quad \mu_{ai} = \sigma_{ai}^2 \left[\frac{(1 - \alpha)\mu_{1i}}{\sigma_{1i}^2} + \frac{\alpha\mu_{2i}}{\sigma_{2i}^2} \right] \quad (36)$$

It is to be noted that the implementation remains the same for both JS^{G_α} and $\text{JS}^{G'_\alpha}$ as given in algorithm 1.

Algorithm 1 Closed form implementation.

Evaluate $JS^{G'_\alpha}$ from Eq. (33)

Evaluate $\mathbb{E}_{q(\mathbf{w}|\theta)} [\log P(\mathbb{D}|\mathbf{w})]$

Sample $\boldsymbol{\varepsilon}_i \sim \mathcal{N}(0, 1); i = 1, \dots, \text{No. of samples}$

$\mathbf{w}_i \leftarrow \boldsymbol{\mu} + \log(1 + \exp(\boldsymbol{\rho})) \circ \boldsymbol{\varepsilon}_i.$

$f_{ll} \leftarrow \sum_i \log P(\mathbb{D}|\mathbf{w}_i)$

Loss:

$$F \leftarrow \lambda JS^{G'_\alpha} - f_{ll}$$

Gradients:

$$\frac{\partial F}{\partial \boldsymbol{\mu}} \leftarrow \sum_i \frac{\partial F}{\partial \mathbf{w}_i} + \frac{\partial F}{\partial \boldsymbol{\mu}}$$

$$\frac{\partial F}{\partial \boldsymbol{\rho}} \leftarrow \sum_i \frac{\partial F}{\partial \mathbf{w}_i} \frac{\boldsymbol{\varepsilon}_i}{1 + \exp(-\boldsymbol{\rho})} + \frac{\partial F}{\partial \boldsymbol{\rho}}$$

Update:

$$\boldsymbol{\mu} \leftarrow \boldsymbol{\mu} - \alpha \frac{\partial F}{\partial \boldsymbol{\mu}}$$

$$\boldsymbol{\rho} \leftarrow \boldsymbol{\rho} - \alpha \frac{\partial F}{\partial \boldsymbol{\rho}}$$

2.5. Minimization of the loss function via Monte Carlo sampling for any general prior

The algorithm provided in the previous subsection 2.4 (algorithm 1) is applicable only when the priors and the posterior distributions are assumed to be Gaussian. To provide a more general algorithm that removes this restriction a Monte Carlo sampling technique can be used to minimize the loss function given in Eq. (31). The expectations in Eq. (31) can be approximated using Monte Carlo samples from the corresponding distributions as shown in the algorithm 2.

2.6. Insights into the advantages of JS divergence-based loss function

To better understand the proposed JS divergence-based loss function, we make use of contrived examples to compare it against the conventional KL divergence-based loss function. In the following we explore two aspects of the proposed loss function:

1. The ability to regularize.
2. The advantage of using the closed-form expression over the Monte Carlo approximation while evaluating the JS divergence.

2.6.1. Regularisation performance

Let two Gaussian distributions $q \sim \mathcal{N}(\mu_1 = \mu, \sigma_1^2 = 0.01)$ and $P \sim \mathcal{N}(\mu_2 = 0, \sigma_2^2 = 0.1)$ mimic the posterior and the prior parameter of the BNN respectively. The closed form divergences for both KL and $JS_{G'_\alpha}$ are evaluated by varying the mean (μ) of the distribution q . This is similar to learning the parameters of the network during training. The values of the divergences are plotted in Fig. 1. It is seen from Fig. 1 that, as the mean of the distribution q (i.e the network parameter) diverges away from the mean of the distribution P (i.e the prior distribution) the JS divergence is much greater as compared to the KL divergence. This implies that the proposed JS divergence-based loss function is penalized higher than the KL divergence-based loss function if the mean of the network parameter is farther away

Algorithm 2 Monte Carlo implementation

Approximate $\mathbb{E}_{q(\mathbf{w}|\theta)}$

 Sample $\boldsymbol{\varepsilon}_i^q \sim \mathcal{N}(0, 1); i = 1, \dots$, No. of samples

$$\mathbf{w}_i^q \leftarrow \boldsymbol{\mu} + \log(1 + \exp(\boldsymbol{\rho})) \circ \boldsymbol{\varepsilon}_i^q.$$

$$c_1 = \lambda(1 - \alpha)^2$$

$$f_1 \leftarrow \sum_i c_1 \log q(\mathbf{w}_i^q|\boldsymbol{\theta}) - c_1 \log P(\mathbf{w}_i^q) - \log P(\mathbb{D}|\mathbf{w}_i^q)$$

Approximate $\mathbb{E}_{P(\mathbf{w})}$

 Sample $\mathbf{w}_j^p \sim P(\mathbf{w}); j = 1, \dots$, No. of samples

$$c_2 = \lambda\alpha^2$$

$$f_2 \leftarrow \sum_j c_2 \log P(\mathbf{w}_j^p) - c_2 \log q(\mathbf{w}_j^p|\boldsymbol{\theta})$$

Loss:

$$F \leftarrow f_1 + f_2$$

Gradients:

$$\frac{\partial F}{\partial \boldsymbol{\mu}} \leftarrow \sum_i \frac{\partial F}{\partial \mathbf{w}_i^q} + \frac{\partial F}{\partial \boldsymbol{\mu}}$$

$$\frac{\partial F}{\partial \boldsymbol{\rho}} \leftarrow \sum_i \frac{\partial F}{\partial \mathbf{w}_i^q} \frac{\boldsymbol{\varepsilon}_i}{1 + \exp(-\boldsymbol{\rho})} + \frac{\partial F}{\partial \boldsymbol{\rho}}$$

Update:

$$\boldsymbol{\mu} \leftarrow \boldsymbol{\mu} - \alpha \frac{\partial F}{\partial \boldsymbol{\mu}}$$

$$\boldsymbol{\rho} \leftarrow \boldsymbol{\rho} - \alpha \frac{\partial F}{\partial \boldsymbol{\rho}}$$

from its prior distribution. Thus, by assuming small means for the priors of the network parameters and finding the right value of α we can regularise the network parameters better in case of the proposed JS divergence-based loss function.

The above example shows that the JS divergence is higher than KL for specific distributions $q \sim \mathcal{N}(\mu_1 = \mu, \sigma_1^2 = 0.01)$ and $P \sim \mathcal{N}(\mu_2 = 0, \sigma_2^2 = 0.1)$ and a given value of $\alpha = 0.5$. For any two arbitrary Gaussian distributions $P \sim \mathcal{N}(\mu_p, \sigma_p^2)$ and $q \sim \mathcal{N}(\mu_q, \sigma_q^2)$, there always exists an $\alpha \in [0, 1]$ such that $\tilde{\mathcal{F}}'_{js} > \mathcal{F}_{KL}$ when $\sigma_p^2 > \sigma_q^2$ as shown below.

2.6.2. Condition for better regularisation

$$\tilde{\mathcal{F}}'_{js} - \mathcal{F}_{KL} > 0 \tag{37a}$$

$$(1 - \alpha)^2 \text{KL}(q||P) + \alpha^2 \text{KL}(P||q) - \text{KL}(q||P) > 0 \tag{37b}$$

$$(\alpha^2 - 2\alpha) \text{KL}(q||P) + \alpha^2 \text{KL}(P||q) > 0 \tag{37c}$$

$$\implies \alpha > \frac{2 \text{KL}(q||P)}{\text{KL}(q||P) + \text{KL}(P||q)} \tag{37d}$$

This is the condition on α for which JS divergence-based loss function regularises better than the KL divergence-based

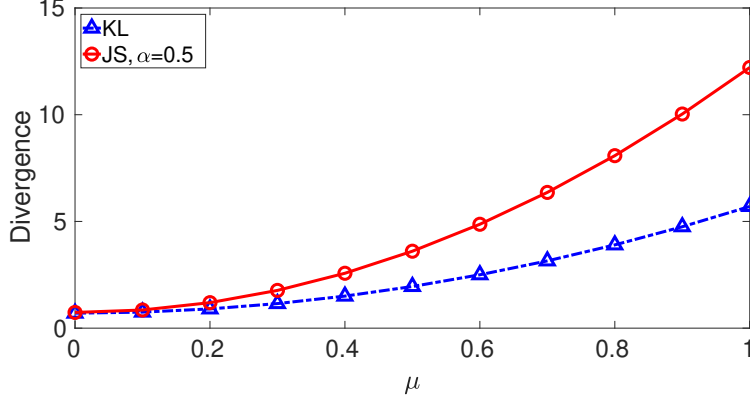


Figure 1: The value of divergence is plotted against the mean μ of q . Since the mean of P is fixed to zero, μ is also the difference in the mean values between the two distributions q and P

loss function. Further,

$$\frac{2 \text{KL}(q||P)}{\text{KL}(q||P) + \text{KL}(P||q)} \geq 0 \quad (38)$$

since KL divergence is always non-negative. Thus,

$$\alpha > \frac{2 \text{KL}(q||P)}{\text{KL}(q||P) + \text{KL}(P||q)} \geq 0 \quad (39)$$

This implies there exists a positive value for α for any P and q such that $\tilde{\mathcal{F}}'_{js}$ is greater than \mathcal{F}_{KL} . Furthermore, $\alpha \in [0, 1]$ implies,

$$1 \geq \alpha > \frac{2 \text{KL}(q||P)}{\text{KL}(q||P) + \text{KL}(P||q)} > 0 \quad (40)$$

To satisfy inequality Eq.(40), we have the condition

$$1 > \frac{2 \text{KL}(q||P)}{\text{KL}(q||P) + \text{KL}(P||q)} \quad (41)$$

$$\implies \text{KL}(P||q) > \text{KL}(q||P) \quad (42)$$

Let, P and q be Gaussian distributions with $P \sim \mathcal{N}(\mu_p, \sigma_p^2)$ and $q \sim \mathcal{N}(\mu_q, \sigma_q^2)$. Then, Eq.(42) can be written as,

$$\ln \frac{\sigma_q^2}{\sigma_p^2} + \frac{\sigma_p^2 + (\mu_q - \mu_p)^2}{\sigma_q^2} - 1 > \ln \frac{\sigma_p^2}{\sigma_q^2} + \frac{\sigma_q^2 + (\mu_p - \mu_q)^2}{\sigma_p^2} - 1 \quad (43)$$

$$\frac{\sigma_p^2}{\sigma_q^2} + \ln \frac{\sigma_q^2}{\sigma_p^2} + \frac{(\mu_q - \mu_p)^2}{\sigma_q^2} - \frac{\sigma_q^2}{\sigma_p^2} + \ln \frac{\sigma_p^2}{\sigma_q^2} + \frac{(\mu_p - \mu_q)^2}{\sigma_p^2} > 0 \quad (44)$$

Let, $\gamma = \frac{\sigma_p^2}{\sigma_q^2}$. Eq.(44) can be rewritten as,

$$\gamma - \frac{1}{\gamma} + \ln \frac{1}{\gamma} - \ln \gamma + \frac{(\mu_q - \mu_p)^2}{\sigma_q^2} - \frac{(\mu_p - \mu_q)^2}{\gamma \sigma_q^2} > 0 \quad (45)$$

$$\gamma - \frac{1}{\gamma} + \ln \frac{1}{\gamma^2} + \frac{(\mu_q - \mu_p)^2}{\sigma_q^2} \left(1 - \frac{1}{\gamma}\right) > 0 \quad (46)$$

This condition Eq.(46) is satisfied when $\gamma > 1$ or

$$\sigma_p^2 > \sigma_q^2 \quad (47)$$

Thus, when P and q are Gaussian distributions with $\sigma_p^2 > \sigma_q^2$, there always exists an $\alpha \in [0, 1]$ such that $\tilde{\mathcal{F}}'_{js} > \mathcal{F}_{KL}$. In other words under these conditions, the JS divergence-based loss function regularises better than the KL divergence-based loss function.

2.6.3. Monte Carlo estimates

A closed-form solution does not exist for KL and JS divergences for most combinations of prior and posterior distributions. In cases where such a closed form for the divergence is unavailable for a given distribution, we can resort to Monte Carlo (MC) estimates. However, estimation of the cost function using MC estimates is computationally expensive. In addition, for networks with a large number of parameters, the memory requirement increases significantly with MC estimates. To estimate the number of MC samples required to achieve the accuracy of closed form estimates, JS divergence of two Gaussian distributions $\mathcal{N}(5, 1)$ and $\mathcal{N}(0, 1)$ are evaluated and compared with its closed form counterpart. Fig. 2 shows the results of the comparison. It is seen that at least 600 samples are required to estimate the JS divergence within 5% error. This implies evaluating the loss function 600 times for a given input and back-propagating the error which requires huge computational efforts. Therefore, utilizing the closed-form solution when available can save huge computational efforts and memory.

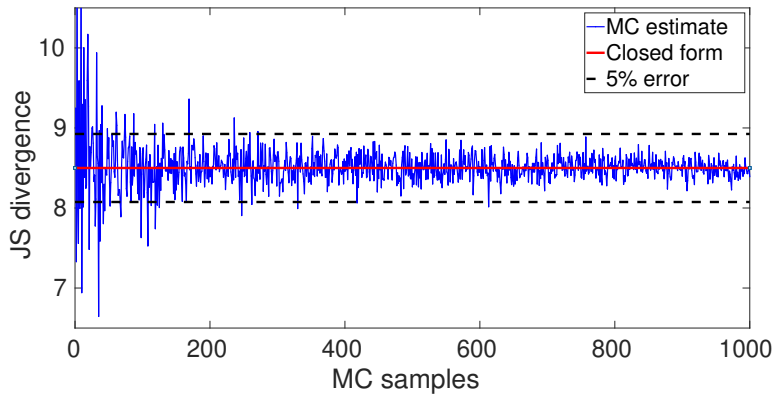


Figure 2: Comparison of MC estimates and the closed form solution of KL divergence demonstrating the benefit of closed form solution.

3. Experiments

To implement the proposed loss function and demonstrate its advantages, we performed experiments and compared them with the existing ELBO loss Eq. (18). The details of the experiments are described in this section. We have used a closed form implementation as proposed in algorithm 1 with the loss function \mathcal{F}'_{js} that utilizes the modified geometric mean in the experiments unless specified otherwise.

3.1. Data sets

Two Data sets were used to perform the experiments namely the CIFAR-10 data set and a publicly available histopathology data set.

3.1.1. CIFAR-10 data set

CIFAR-10 data set consists of 60,000 images of size $32 \times 32 \times 3$ belonging to 10 mutually exclusive classes. This dataset is an unbiased dataset with each of the 10 classes having 6,000 images.

Images were normalized using the min-max normalization technique. To demonstrate the effectiveness of regularisation, varying levels of Gaussian noise were added to the normalized CIFAR-10 data set. The entire dataset was split into 60%-20%-20% for training-validation-testing respectively. Two Bayesian CNNs with the same architecture were trained by: 1) minimizing the ELBO loss Eq. (18), and 2) minimising the proposed loss function \mathcal{F}'_{js} in Eq. (30).

3.1.2. Histopathology data set

To demonstrate the effectiveness of the loss function on a biased data set, we used a publicly available breast histopathology data set [34]. These are images containing regions of Invasive Ductal Carcinoma. The original data set consisted of 162 whole mount slide images of Breast Cancer specimens scanned at 40x. From the original whole slide images, 277,524 patches of size $50 \times 50 \times 3$ pixels were extracted (198,738 negative and 78,786 positive), labeled by pathologists, and provided as a data set for classification.

The data set consists of two classes: positive (1) and negative (0). 20% of the entire data set was used as the testing set for our study. The remaining 80% of the entire data was further split into a training set and a validation set (80%-20% split) to perform hyperparameter optimization. The images were shuffled and converted from uint8 to float format for normalizing. As a post-processing step, we computed the complement of all the images (training and testing) and then used them as inputs to the neural network. The pixel-wise normalization and complement was carried out as $p_n = (255 - p)/255$. Where p is the original pixel value and p_n is the pixel value after normalization and complement.

3.2. Hyperparameter optimisation and network Architecture

Hyperparameters for all the networks considered here are chosen through hyperparameter optimization. A Tree-structured Parzen Estimator (TPE) algorithm is used which is a sequential model-based optimization approach [35]. In this approach, models are constructed to approximate the performance of hyperparameters based on historical measurements. New hyperparameters are chosen based on this model to evaluate performance. A python library Hyperopt [36] is used to implement this optimization algorithm over a given search space. Data is split into a training set and a validation set as explained in section 3.1. An optimization is performed to maximize the validation accuracy for different hyperparameter settings of the network.

The architecture of all the networks used in this work follows the ResNet-18 V1 model [37] without the batch normalization layers. The network parameters are initialized with the weights of ResNet-18 trained on the Imagenet data set[38]

4. Results and discussions

This section presents the classification results on the noisy CIFAR and the biased histopathology data sets. A comparison of the performance is presented between the existing KL divergence-based loss function and the JS divergence-based loss function proposed in this work.

4.1. Results of hyperparameter optimisation

Results of the hyperparameter optimisation (described in Section. 3.2) for the two data sets are presented in Tables. 1 and 2.

It is to be noted that in the case of the JS divergence-based loss function proposed in this work, the additional parameter α is optimized along with the learning rate for each training data set.

4.2. Training and Validation

The data set was split into a training, a validation, and a test set as explained in Section. 3.1. Training of the networks is done until the loss converges or the validation accuracy starts to decrease. The test results provided in the upcoming sections correspond to the epoch in which the validation accuracy was maximum.

Table 1: CIFAR10 dataset

Noise level (σ)	0.1	0.2	0.3	0.4	0.5
α	0.004	0.1313	0.2855	0.3052	0.2637
Learning rate (JS)	1e-4	1e-4	1e-4	1e-4	1e-5
Learning rate (KL)	1e-4	1e-4	1e-4	1e-3	1e-3

Noise level (σ)	0.6	0.7	0.8	0.9	
α	0.2249	0.3704	0.3893	0.7584	
Learning rate (JS)	1e-4	1e-4	1e-5	1e-3	
Learning rate (KL)	1e-3	1e-3	1e-3	1e-3	

Table 2: Histopathology dataset

Divergence	α	Learning rate
JS	0.0838	1e-4
KL	-	1e-4

4.2.1. CIFAR 10

Training of the CIFAR 10 dataset is performed with varying levels of noise intensity. Accuracy of training and validation sets for noise $\mathcal{N}(\mu = 0, \sigma = 0.9)$ is presented for both KL divergence based loss function and the proposed JS divergence based loss function in Fig. 3. It is observed from Fig. 3 that KL divergence-based loss function over-

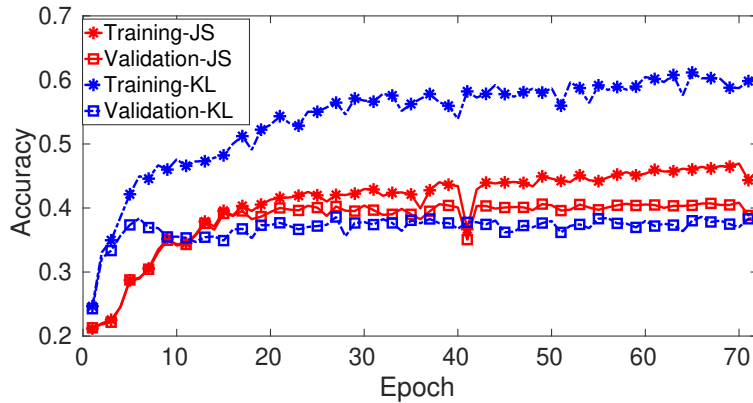


Figure 3: Training and validation of CIFAR 10 dataset with added Gaussian noise $\mathcal{N}(\mu = 0, \sigma = 0.9)$ using the KL-loss function and the proposed JS divergence based loss function.

fits the training data by learning the noise whereas the JS divergence-based loss regularises better showing better generalization for the unseen validation dataset. The JS divergence-based loss function also provides better results in terms of accuracy in classifying validation and test sets. Although a representative case of $\sigma = 0.9$ is presented here, a similar trend was observed for other noise levels as well.

4.2.2. Histopathology

Training of the histopathology dataset is performed using the hyperparameters obtained in Table 2. Fig. 4 shows the accuracy of training and validation sets for the KL divergence-based loss function and the proposed JS divergence-based loss function. Similar to the noisy CIFAR-10 data set, the KL divergence-based loss function learns the training data too well and fails to generalize for the unseen validation set. Whereas, the proposed JS divergence-based loss function regularises better and provides more accurate results for the validation and test sets.

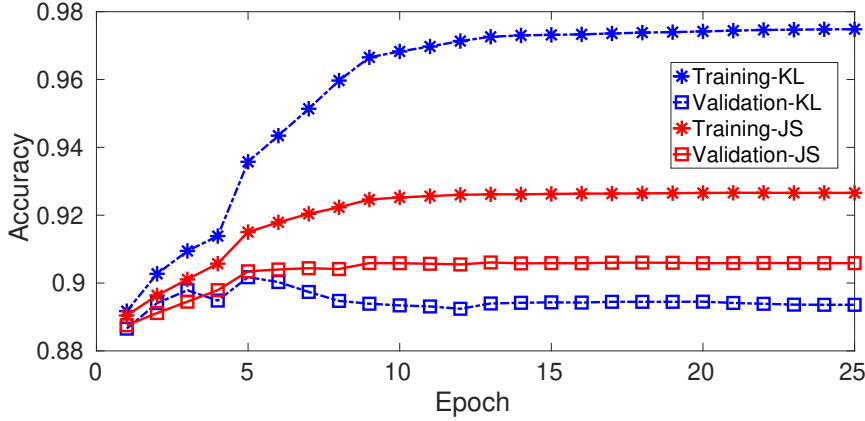


Figure 4: Training and validation of histopathology dataset using the KL-loss function and the proposed JS divergence-based loss function.

4.3. Testing

Results obtained on the test sets of noisy CIFAR-10 data sets and the histopathology data set are presented in this section. Five runs were performed with different mutually exclusive training and validation tests to compare the results of the KL divergence-based loss function and the proposed JS divergence-based loss function.

4.3.1. CIFAR 10

The accuracy of the noisy CIFAR 10 test data set at varying noise levels is presented in Fig. 5 and Fig. 6. It

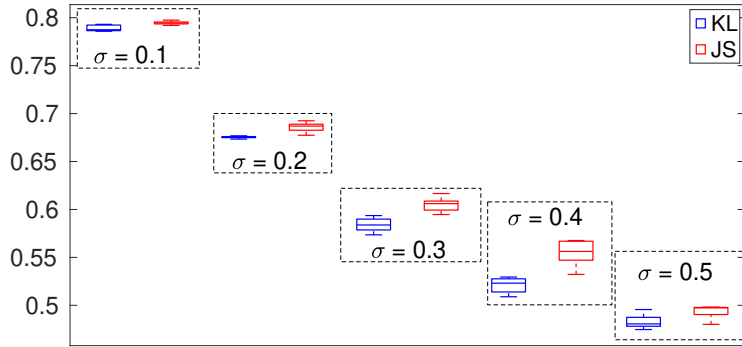


Figure 5: Accuracy on the test data set at different noise levels (from $\sigma = 0.1$ to $\sigma = 0.5$). Each box chart displays the median as the center line, the lower and upper quartiles as the box edges, and the minimum and maximum values as whiskers.

is observed from Fig. 5 and Fig. 6 that the accuracy of the proposed JS divergence-based loss function is better in all the noise level cases. It is also seen that the difference in accuracy between KL divergence-based loss and the JS divergence-based loss increases with increasing noise levels. This demonstrates the regularising capability of the proposed JS divergence-based loss function.

To further evaluate the performance of the proposed method, confusion matrices for one of the five runs for both KL based loss function and the proposed JS divergence-based loss function are shown in Fig.7

4.3.2. Histopathology

Five runs were performed with different training and validation tests to compare the results of the KL divergence-based loss function and the proposed JS divergence-based loss function on the biased histopathology data set. It

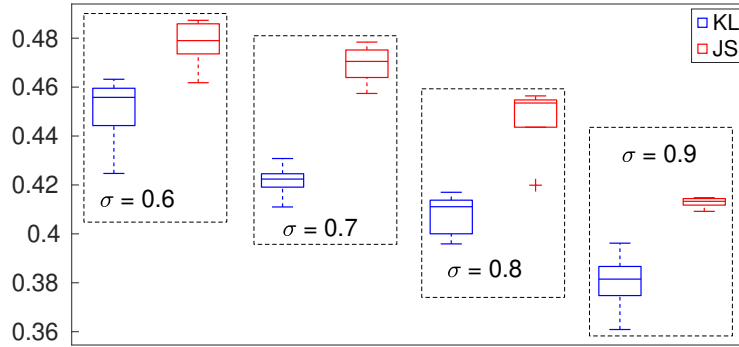


Figure 6: Accuracy on the test data set at different noise levels (from $\sigma = 0.6$ to $\sigma = 0.9$) Each box chart displays the median as the center line, the lower and upper quartiles as the box edges, and the minimum and maximum values as whiskers.

	airplane	853	5	35	8	8	8	5	10	60	8	
	automobile	14	879	3	5	2	3	5	3	39	47	
	bird	49	5	685	31	69	78	55	14	13	1	
	cat	24	2	56	541	39	216	60	36	18	8	
	deer	15	0	45	49	722	67	36	52	12	2	
	dog	8	2	31	87	29	777	26	34	4	2	
	frog	6	1	38	42	25	49	827	3	8	1	
	horse	14	0	17	27	47	61	6	817	8	3	
	ship	35	8	10	6	3	5	4	4	915	10	
	truck	17	59	9	9	1	10	4	10	40	841	
True labels		airplane	automobile	bird	cat	deer	dog	frog	horse	ship	truck	
		Predicted labels										

(a) KL

	airplane	815	18	35	19	14	2	6	23	52	16	
	automobile	4	915	5	4	2	2	1	6	10	51	
	bird	42	4	680	66	68	39	40	47	7	7	
	cat	11	7	48	697	43	75	33	67	9	10	
	deer	10	1	66	68	728	12	25	82	6	2	
	dog	3	3	36	163	32	656	19	78	4	6	
	frog	6	1	53	76	37	16	784	13	6	8	
	horse	8	0	16	25	31	14	3	897	1	5	
	ship	29	18	10	11	10	3	3	8	894	14	
	truck	15	66	4	15	4	3	1	15	16	861	
True labels		airplane	automobile	bird	cat	deer	dog	frog	horse	ship	truck	
		Predicted labels										

(b) JS

Figure 7: Confusion matrices for (a) KL divergence-based loss function and (b) proposed JS divergence-based loss function on the noisy CIFAR-10 data set.

is evident from Fig. 8 that the proposed JS divergence-based loss function performs better than the existing KL divergence-based loss function in all five runs with different training and validation sets. Since this data set is biased toward the negative class, the improvement in performance shown by the proposed JS divergence-based loss function is attributed to better regularisation and generalization capabilities of the loss function. The receiver operating characteristic (ROC) curve is a performance evaluation metric that visually plots the classification ability of a binary classifier when the discrimination threshold is varied. For this binary classification problem on histopathology data set the ROC curve is plotted in Fig. 9. It is seen from the values of the area under the curve (AUC) that the proposed JS divergence-based loss function performs better than the existing KL divergence-based loss function.

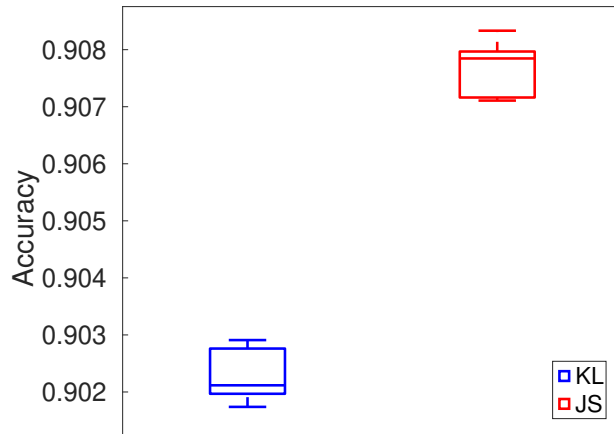


Figure 8: Accuracy on the test data set for five runs. Each box chart displays the median as the center line, the lower and upper quartiles as the box edges, and the minimum and maximum values as whiskers.

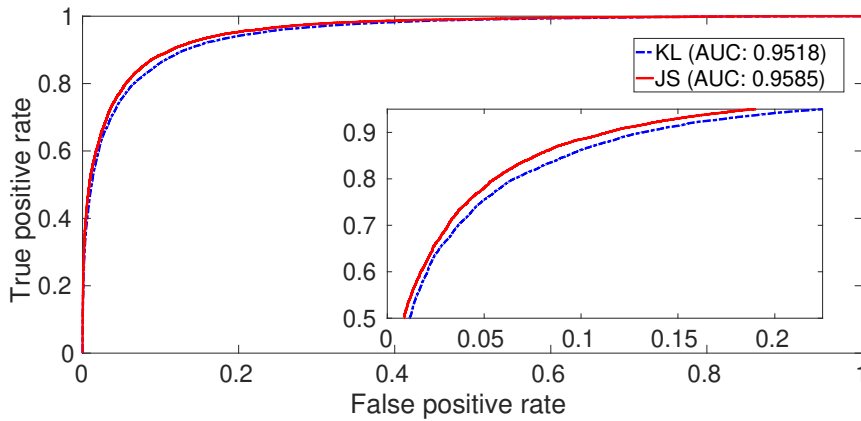


Figure 9: Receiver operating characteristic curve depicting the classification performance of the two binary classifiers studied.



Figure 10: Confusion matrices for (a) KL divergence based loss function and (b) JS divergence based loss function on the histopathology data set.

Confusion matrices for the proposed JS divergence-based loss function and the existing KL divergence-based loss function are shown in Fig.10. It is observed from Fig. 10 that in addition to improving the accuracy of predictions, the proposed JS divergence-based loss function reduced the number of false negative predictions by 11.7% as compared to the existing KL divergence-based loss function. Given that the data set is biased towards the negative class, this is a significant achievement.

5. Conclusions

In this study, we introduced a novel JS divergence-based loss function for Bayesian neural networks that extends the state-of-the-art loss functions. The proposed loss function generalizes well for noisy and biased data sets. To conclude this study, we summarise its main findings as follows.

Firstly, we have formulated a JS Divergence based loss function for Bayesian neural networks and have shown that this is a generalization of the widely used KL divergence-based loss function.

Secondly, we have derived the conditions to obtain better regularisation through the proposed JS divergence-based loss function for Gaussian priors and posteriors.

Thirdly, we have provided algorithms for the closed form evaluation as well as the Monte Carlo approximation of the proposed loss function. The relative merits of these two approaches are discussed.

Fourthly, we have shown the improvement in performance achieved by the proposed loss function in terms of various performance metrics on data sets having bias and various degrees of noise.

This work would serve as a foundation for the exploration of other divergences for variational inferences in machine learning models.

References

- [1] G. Litjens, T. Kooi, B. E. Bejnordi, A. A. A. Setio, F. Ciompi, M. Ghafoorian, J. A. Van Der Laak, B. Van Ginneken, and C. I. Sánchez, "A survey on deep learning in medical image analysis," *Medical image analysis*, vol. 42, pp. 60–88, 2017.
- [2] D. Shen, G. Wu, and H.-I. Suk, "Deep learning in medical image analysis," *Annual review of biomedical engineering*, vol. 19, p. 221, 2017.
- [3] P. Thiagarajan, P. Khairnar, and S. Ghosh, "Explanation and use of uncertainty quantified by bayesian neural network classifiers for breast histopathology images," *IEEE Transactions on Medical Imaging*, vol. 41, no. 4, pp. 815–825, 2021.
- [4] M. Frank, D. Drikakis, and V. Charissis, "Machine-learning methods for computational science and engineering," *Computation*, vol. 8, no. 1, p. 15, 2020.
- [5] S. Kollmannsberger, D. D'Angella, M. Jokeit, L. Herrmann, *et al.*, *Deep Learning in Computational Mechanics*. Springer, 2021.
- [6] U. Yadav, S. Pathrudkar, and S. Ghosh, "Interpretable machine learning model for the deformation of multiwalled carbon nanotubes," *Physical Review B*, vol. 103, no. 3, p. 035407, 2021.
- [7] K. Choudhary, B. DeCost, C. Chen, A. Jain, F. Tavazza, R. Cohn, C. W. Park, A. Choudhary, A. Agrawal, S. J. Billinge, *et al.*, "Recent advances and applications of deep learning methods in materials science," *npj Computational Materials*, vol. 8, no. 1, pp. 1–26, 2022.
- [8] S. Pathrudkar, H. M. Yu, S. Ghosh, and A. S. Banerjee, "Machine learning based prediction of the electronic structure of quasi-one-dimensional materials under strain," *Physical Review B*, vol. 105, no. 19, p. 195141, 2022.
- [9] C. Beck, M. Hutzenhaler, A. Jentzen, and B. Kuckuck, "An overview on deep learning-based approximation methods for partial differential equations," *arXiv preprint arXiv:2012.12348*, 2020.
- [10] R. Matthey and S. Ghosh, "A novel sequential method to train physics informed neural networks for allen cahn and cahn hilliard equations," *Computer Methods in Applied Mechanics and Engineering*, vol. 390, p. 114474, 2022.
- [11] M. Buda, A. Maki, and M. A. Mazurowski, "A systematic study of the class imbalance problem in convolutional neural networks," *Neural Networks*, vol. 106, pp. 249–259, 2018.
- [12] H. D. Kabir, A. Khosravi, M. A. Hosen, and S. Nahavandi, "Neural network-based uncertainty quantification: A survey of methodologies and applications," *IEEE access*, vol. 6, pp. 36218–36234, 2018.
- [13] L. V. Jospin, H. Laga, F. Boussaid, W. Buntine, and M. Bennamoun, "Hands-on bayesian neural networks—a tutorial for deep learning users," *IEEE Computational Intelligence Magazine*, vol. 17, no. 2, pp. 29–48, 2022.
- [14] N. Tishby, E. Levin, and S. A. Solla, "Consistent inference of probabilities in layered networks: Predictions and generalization," in *International Joint Conference on Neural Networks*, vol. 2, pp. 403–409, IEEE New York, 1989.
- [15] J. Denker and Y. LeCun, "Transforming neural-net output levels to probability distributions," *Advances in neural information processing systems*, vol. 3, 1990.
- [16] E. Goan and C. Fookes, *Bayesian Neural Networks: An Introduction and Survey*, pp. 45–87. Cham: Springer International Publishing, 2020.
- [17] Y. Gal *et al.*, "Uncertainty in deep learning," 2016.
- [18] G. E. Hinton and D. Van Camp, "Keeping the neural networks simple by minimizing the description length of the weights," in *Proceedings of the sixth annual conference on Computational learning theory*, pp. 5–13, 1993.
- [19] D. Barber and C. M. Bishop, "Ensemble learning in bayesian neural networks," *Nato ASI Series F Computer and Systems Sciences*, vol. 168, pp. 215–238, 1998.
- [20] R. M. Neal, *Bayesian learning for neural networks*, vol. 118. Springer Science & Business Media, 2012.
- [21] M. Welling and Y. W. Teh, "Bayesian learning via stochastic gradient langevin dynamics," in *Proceedings of the 28th international conference on machine learning (ICML-11)*, pp. 681–688, Citeseer, 2011.
- [22] A. Graves, "Practical variational inference for neural networks," *Advances in neural information processing systems*, vol. 24, 2011.
- [23] J. M. Hernández-Lobato and R. Adams, "Probabilistic backpropagation for scalable learning of bayesian neural networks," in *International conference on machine learning*, pp. 1861–1869, PMLR, 2015.
- [24] C. Blundell, J. Cornebise, K. Kavukcuoglu, and D. Wierstra, "Weight uncertainty in neural network," in *International conference on machine learning*, pp. 1613–1622, PMLR, 2015.
- [25] D. P. Kingma and M. Welling, "Auto-encoding variational bayes," *arXiv preprint arXiv:1312.6114*, 2013.

- [26] D. J. Rezende, S. Mohamed, and D. Wierstra, “Stochastic backpropagation and approximate inference in deep generative models,” in *International conference on machine learning*, pp. 1278–1286, PMLR, 2014.
- [27] J. Hensman, M. Zwießebele, and N. D. Lawrence, “Tilted variational bayes,” in *Artificial Intelligence and Statistics*, pp. 356–364, PMLR, 2014.
- [28] J. Hernandez-Lobato, Y. Li, M. Rowland, T. Bui, D. Hernandez-Lobato, and R. Turner, “Black-box alpha divergence minimization,” in *Proceedings of The 33rd International Conference on Machine Learning* (M. F. Balcan and K. Q. Weinberger, eds.), vol. 48 of *Proceedings of Machine Learning Research*, (New York, New York, USA), pp. 1511–1520, PMLR, 20–22 Jun 2016.
- [29] Y. Li and R. E. Turner, “Rényi divergence variational inference,” *Advances in neural information processing systems*, vol. 29, 2016.
- [30] T. Minka *et al.*, “Divergence measures and message passing,” tech. rep., Microsoft Research, 2005.
- [31] F. Nielsen, “On the jensen–shannon symmetrization of distances relying on abstract means,” *Entropy*, vol. 21, no. 5, p. 485, 2019.
- [32] J. Deasy, N. Simidjievski, and P. Liò, “Constraining variational inference with geometric jensen-shannon divergence,” *Advances in Neural Information Processing Systems*, vol. 33, pp. 10647–10658, 2020.
- [33] I. Higgins, L. Matthey, A. Pal, C. Burgess, X. Glorot, M. Botvinick, S. Mohamed, and A. Lerchner, “beta-vae: Learning basic visual concepts with a constrained variational framework,” 2016.
- [34] Paul Mooney, “Breast Histopathology Images.” <https://www.kaggle.com/paultimothymooney/breast-histopathology-images>. 2017.
- [35] J. Bergstra, R. Bardenet, Y. Bengio, and B. Kégl, “Algorithms for hyper-parameter optimization,” in *25th annual conference on neural information processing systems (NIPS 2011)*, vol. 24, Neural Information Processing Systems Foundation, 2011.
- [36] J. Bergstra, D. Yamins, and D. Cox, “Making a science of model search: Hyperparameter optimization in hundreds of dimensions for vision architectures,” in *International conference on machine learning*, pp. 115–123, PMLR, 2013.
- [37] K. He, X. Zhang, S. Ren, and J. Sun, “Deep residual learning for image recognition,” in *Proceedings of the IEEE conference on computer vision and pattern recognition*, pp. 770–778, 2016.
- [38] A. Krizhevsky, I. Sutskever, and G. E. Hinton, “Imagenet classification with deep convolutional neural networks,” in *Advances in neural information processing systems*, pp. 1097–1105, 2012.